Invited paper

OPTO-ELECTRONICS REVIEW **8**(2), 83–90 (2000)

Simulation of optical phenomena in vertical-cavity surface-emitting lasers I. Fundamental principles

W. NAKWASKI*

Institute of Physics, Technical University of Łódź
219 Wólczańska Str., 93-005 Łódź, Poland
and
Centre for High Technology Materials, University of New Mexico
Albuquerque, NM 87106, 1313 Goddard SE, USA

In the present paper, the fundamental principles of simulations of optical phenomena taking place in vertical-cavity surface-emitting lasers (VCSELs) are presented. Polarisation properties of their radiation are shown to justify possibility of an application of the simple scalar Maxwell equation in simplified modelling of standard VCSELs. In the case of microresonator lasers as well as in more exact modelling of a VCSEL operation, however, the full vector approaches are necessary to be applied. They require solving six wave equations with six unknown components of both the $\bar{E}$ and $\bar{H}$ vectors, which needs much more involved solving approaches as well as more computer memory and more CPU time to be implemented. Some interactions between optical and other physical phenomena inside VCSEL resonators are also described. They are shown to play an essential role in the whole VCSEL operation and can not be neglected in their more advanced simulations. Their role is especially important in highly excited VCSELs when many physical phenomena (optical, electrical, thermal and other processes) taking place inside VCSELs volumes during their operation are strongly interrelated with one another.

Keywords: vertical-cavity surface-emitting lasers (VCSELs), optical models, simulation approaches Maxwell equations.

1. Introduction

At present vertical-cavity surface-emitting lasers (VCSELs) are undoubtedly the most advanced designs of semiconductor injection lasers. Since the very beginning they have been generating considerable interest due to a number of unique features that distinguish them from conventional and well-known edge-emitting lasers (EELs). The most essential features include [1] inherent dynamic single-longitudinal-mode operation (owing to the short optical cavity length), presence of high-reflectivity mirrors necessary to compensate for the short length of the active medium, low-divergence non-astigmatic circular output beam, device geometry suitable for integration into two-dimensional (2D) arrays or for monolithic integration with electronic devices, compatibility with vertical-stacking architecture, and so on.

VCSEL designs, however, are still far from being optimal. For example, their continuous-wave (CW) operation and their integration scale are still seriously limited by their thermal behaviour, thermal resistances and series electrical resistances of VCSELs are usually relatively high and higher-order transverse modes are often easily excited just over thresholds. Therefore they still need structure modifications to improve their performance characteristics and to follow earlier development of EELs. This may be carried out using the so-called trial-and-error method. Much more efficient way, however, is to apply computer simulation of their laser operation using methods of computer physics. Such a simulation would enable us to understand better physical phenomena taking place inside a VCSEL volume during its operation in the whole complexity of many nonlinear and mutual interactions between individual physical processes. It could be also used to analyse a relative influence of various device configurations and material parameters of the laser design under consideration on its operation characteristics. Therefore it would be helpful in identifying parameters which are crucial for efficient laser performance and in finding means of its improving.

VCSELs modelling is a very involved task because of their multilayered structure (sometimes containing as many as over a hundred layers), often of nonplanar or buried-type designs, with many heterojunctions, graded layers, strained layers, single or multiple quantum wells, superlattices, oxide and/or oxidised layers, barriers, etched wells, mushroom structures or mesas etc. Therefore in advanced VCSEL models, all material and structure parameters should be used as functions of local material compositions. Additionally, physical phenomena taking place during an operation of a diode laser are mutually interrelated. Electrical phenomena affect optical phenomena and vice versa

*e-mail: nakwaski@ck-sg.p.lodz.pl

and the analogous interactions take place between various thermal phenomena and electrical ones as well as between thermal phenomena and optical ones. Besides all the above phenomena are also influenced by mechanical, chemical, photochemical processes and so on. Therefore comprehensive simulations of a diode laser operation need self-consistency parts including important interrelations between individual physical phenomena. The above means that, in such simulations, the material and structure parameters should be also dependent on local conditions, i.e., temperature increases, carrier concentrations, radiation intensities, electric fields, etc. These self-consistency parts are especially important in modelling of VCSELs which are usually working at much higher excitation level than conventional EELs, so nonlinear interrelations between physical phenomena become much stronger.

To model VCSEL operation, all important and often mutually interrelated physical phenomena (optical, electrical, thermal ones, etc.) taking place within its volume should be correctly included. From among them, the most involved are optical phenomena together with their interactions with matter (gain and absorption, reflection, refraction, focusing, scattering etc.). Therefore this paper is devoted to presenting basics of optical processes essential for a VCSEL operation. They may be used in optical parts of advanced VCSEL models. The paper is organised as follows. VCSEL structures are briefly described in Section 2. Polarisation effects in VCSELs are reviewed in Section 3. Section 4 introduces the Maxwell equations and their application to optical VCSEL modelling. More important interactions between optical processes and other physical phenomena are shown in Section 5. The steady-state solution is introduced in Section 6 that is followed by the conclusions in Section 7. The second part [2] of this paper will present optical VCSEL models known from scientific literature.

2. VCSEL structures

Principally all semiconductor laser devices operate in a similar way and may be described using analogous relations. But there is an essential structural difference between EELs and VCSELs. As one can see in Fig. 1, stimulated radiation travelling in EELs between resonator mirrors is propagated in the plane parallel to the p-n junction remaining in the laser resonator always within its active region, whereas it travels in the direction perpendicular to the p-n junction plane in VCSEL resonators, being amplified inside their active regions during only a small part of the round trip.

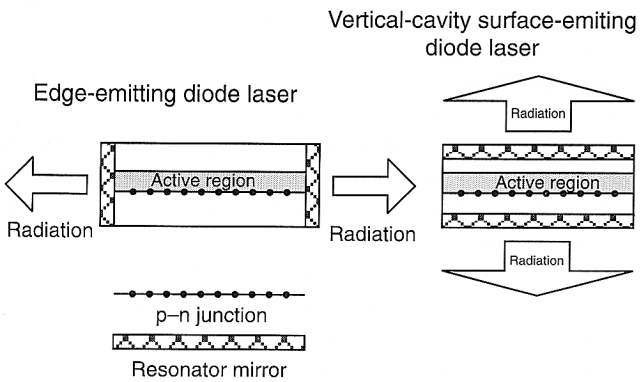

Fig. 1. Schematic configurations of EELs and of VCSELs.

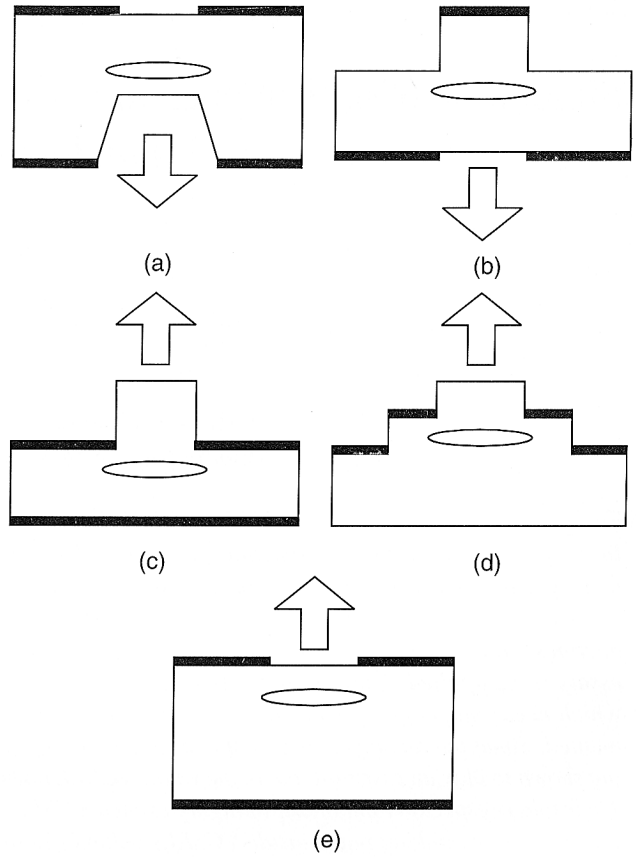

Fig. 2. Basic structures of VCSELs: (a) etched-well laser, (b) back-emitting post laser, (c) lateral-injection post laser, (d) double-lateral-injection post laser, and (e) planar top-emitting laser.

Two important consequences follow from these peculiarities of the VCSEL configuration. First of all, during one round trip, gain is provided to radiation much less effectively in VCSELs than in EELs; therefore in VCSELs its local value inside the active region must usually be higher and radiation losses must be drastically reduced to achieve a lasing threshold as compared to the situation in EELs. The latter requirement is mainly accomplished by manufacturing VCSEL resonator mirrors of much higher reflectivities (very close to unity) than in standard EELs. The second consequence of VCSEL configurations is connected with their much shorter resonator lengths than in EELs, which is followed by much larger mode separations on laser spectral characteristics. For that reason, several longitudinal modes usually coincide with the gain peak in EELs, whereas in VCSELs only one (if any) is within the spectral gain bandwidth. Therefore VCSELs are inherently dynamical single-longitudinal-mode devices.

Some basic VCSEL structures are schematically shown in Fig. 2. Generally, most of them may be divided into etched-well VCSELs [for which the first room-temperature (RT) continuous-wave (CW) operation was reported [3]], post VCSELs (including lateral-injection VCSELs) and very popular planar top-emitting VCSELs (mostly proton-implanted top-surface-emitting lasers – PITSELs). Many other VCSEL configurations have been also reported. Their peculiar contact and mirror geometries depend also on a direction of output beams (back-emitting or top-emitting VCSELs). In Fig. 2, only localisation of VCSEL active regions (as ellipses) and contacts (as black areas) is given. Details concerning a current flow, a carrier confinement as well as waveguiding properties depend on a specific VCSEL design and technology used therefore they are omitted in these schematic pictures. Much more complete review of specific VCSEL constructions is presented in Ref. 4.

3. Polarisation effects

Standard VCSELs grown on typical (100)-oriented substrates are reported to emit light linearly TE polarised in the plane perpendicular to the direction of laser emission just over their lasing thresholds [5–8]. Their emission is switched to the orthogonal linear polarisation when the operation current is increased [7,8] with the same transverse optical mode. Lasing power in the fundamental VCSEL transverse mode is distributed between both orthogonal TE polarisation states [8] giving a considerable partitioning noise between them [9,10]. Orientation of those linearly polarised emissions may be either randomly situated in the above plane [5,8] or may coincide with the <011> and <01$\bar{1}$> crystal axes [9,11]. The last case may lead to birefringence (double refraction) phenomena and to different reflectivities of both the emissions at the resonator mirrors [12,13]. Even more complicated behaviours involving higher order transverse modes and polarisation state changes have been observed at higher operation currents [6,8,14].

VCSELs exhibiting stable polarisation operation are, however, still desirable in many various polarisation-sensitive applications, including low noise, high bit rate data transmission systems [15], smart-pixel-based free space optical interconnects using polarisation-dependent optical components like a polarisation beam splitter and magneto-optics disk computer memories. Polarisation control may be easily accomplished in VCSELs grown on (311) substrates [16] because of a distinct anisotropy of gain in their active regions [17–21]. Other methods take advantage of coating on the sides of the upper DBR mirror which introduces differential optical losses [22], of gain anisotropy in VCSELs [23] (accomplished using strain-related gain in structures with an elliptical hole etched in the substrate [24,25] or in structurally anisotropic self-assembled quantum dots [26]), and of the anisotropic (rectangular, elliptical, zigzag-sidewall or cruciform) transverse geometry of the VCSEL cavities [9,23,27–30].

4. The Maxwell equations

Because of the above polarisation effects, scalar approaches to optical phenomena in standard VCSELs usually seem to be suitable enough unless output polarisation should be determined or stress-related anisotropic phenomena are to be included. Such scalar models are proved to work well in relatively simple VCSEL structures. Comprehensive analyses of more complex VCSEL designs, however, need more involved vectorial approaches, which, however, have common disadvantage of requiring extensive computing resources for their implementation. But on the other hand, fully vectorial optical simulations may additionally improve model exactness by introducing e.g. anisotropic polarisation-related phenomena into the analysis [31–36].

VCSEL configurations exhibit unique possibility to reduce their lasing thresholds simply by reducing a radial size of their active regions (microresonator lasers). Technologically it is achievable for example with the aid of selective oxidation of AlAs layers introduced below and/or above the layer (containing an active region in its central part) to leave unaffected only a very small central aperture of partly oxidised layers. In such microresonator lasers, the spontaneous emission factor β_{sp} (describing the fraction of spontaneous emission coupled into lasing modes) is expected to increase [37,38] which is followed by less sharp curving of light-current characteristics at threshold [39]. The transverse dimensions shrink of VCSEL microresonators to the order of the lasing wavelength is followed by a distinct curving of spatial mode profiles which can not be treated as plane waves any more. So, in this case, simplified scalar approaches to optical field modelling may lead to incorrect results, hence more complete vectorial analyses should be applied (e.g. [40]).

Generally, the optical field properties are governed by the Maxwell equations, which, for a source-free case and the assumed $\exp(-i\omega t)$ time dependencies of both the electric field vector $\vec{E}$ and the magnetic field vector $\vec{H}$, may be written in the following form [41]

$$\nabla \times \vec{H} = -i\omega\varepsilon\vec{E}, \tag{1}$$

$$\nabla \times \vec{E} = i\omega\mu\vec{H}, \tag{2}$$

$$\nabla \cdot (\varepsilon\vec{E}) = 0, \tag{3}$$

$$\nabla \cdot (\mu\vec{H}) = 0, \tag{4}$$

where i stands for the imaginary unit, ε is the dielectric constant, μ is the magnetic permeability, ω stands for the circular frequency of an electromagnetic wave, and ∇ is the Nabla operator, becoming the curl (as $\nabla\times$) and the divergent (as $\nabla\cdot$) operators. For nonmagnetic materials, which normally constitute volumes of semiconductor lasers, the magnetic permeability μ is very nearly equal to the free-space value μ_0. The dielectric constant ε, on the other hand, is related to the refractive index n_R by

$$\varepsilon(x,y,z) = n_R^2(x,y,z)\varepsilon_0, \tag{5}$$

where ε_0 is the dielectric constant of free space. Both ε_0 and μ_0 are interrelated via the speed of light c in vacuum

$$c = (\varepsilon_0\mu_0)^{-1/2}. \tag{6}$$

For homogeneous lossless medium, the Maxwell equations (1–4) may be combined to give the vector wave equations

$$(\nabla^2 + k_0^2 n_R^2)\vec{\psi} = 0, \tag{7}$$

where ∇^2 is the vector Laplacian, $k_0 = \omega/c$ is the wave number, and $\vec{\psi}$ may be either $\vec{E}$ or $\vec{H}$ vectors. Equation (7) is approximately satisfied also in inhomogeneous media, provided that along a distance equal to the wavelength $\lambda = 2\pi c/\omega$ the dielectric constants change by less than unity [42].

Using the expansion of the vector Laplacian

$$\nabla^2\vec{\psi} = \vec{1}_x \Delta\Phi_x + \vec{1}_y \Delta\Phi_y + \vec{1}_z \Delta\Phi_z, \tag{8}$$

where Δ is the scalar Laplacian, $\vec{1}_x$, $\vec{1}_y$ and $\vec{1}_z$ are the corresponding unit vectors, and Φ_x, Φ_y and Φ_z represent scalar components of the $\vec{E}$ or the $\vec{H}$ vectors, the vector equation (7) may be easily reduced to the following scalar wave equations (for i = x, y, z)

$$(\Delta + k_0^2 n_R^2)\Phi_i = 0, \tag{9}$$

for each Φ_i component of $\vec{E}$ and $\vec{H}$ vectors.

In lossy (or gain) media, instead of the real index of refraction n_R in Eqs. (7) and (9), the complex index of refraction N_R

$$N_R = n_R - ik_e, \tag{10}$$

is rather used, where k_e is the extinction coefficient. Then both the vector (7) and the scalar (9) wave equations may be written in the following forms

$$(\nabla^2 + k_0^2 N_R^2)\vec{\psi} = 0, \tag{11}$$

$$(\Delta + k_0^2 N_R^2)\Phi_i = 0, \tag{12}$$

and their solutions becomes complex quantities.

The extinction coefficient is directly related to the absorption α coefficient

$$k_e = \frac{\alpha}{2k_0}. \tag{13}$$

It should be remembered, that the above relation remains valid also for "negative" absorption, i.e., for gain: $g = -\alpha$.

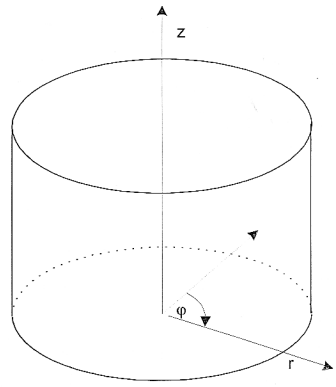

Fig. 3. The cylindrical (z,r,φ) co-ordinate system used in modelling of optical processes in VCSELs.

Because of a distinct cylindrical symmetry of most of VCSEL devices, from now on the cylindrical (r,z,φ) co-ordinate system is used (see Fig. 3), with z directed along the symmetry axis, r perpendicular to it and φ is the azimuthal angle. So, consequently, the radiation longitudinal modes (with different nodes and anti-nodes numbers along the resonator length 0z), the radiation azimuthal modes (with different analogous numbers around the symmetry axis), and the radiation transverse modes (with different analogous numbers along the radial direction) will be distinguished.

5. Interactions with other physical phenomena

Optical phenomena are interrelated with other physical phenomena taking place inside a VCSEL volume, especially with electrical and thermal ones. Therefore optical processes should not be analysed separately. Many of these interactions are described by coupled rate equations for the carrier concentration n (called also the continuity equation) and for the photon densities $S_{k,m,s}$ in each k^{th} azimuthal mode, m^{th} transverse mode and the s^{th} longitudinal mode, which may be written in the following form

$$\frac{\delta n}{\delta t} = (G - R) + \frac{1}{r}\frac{\partial}{\partial r}\left(D_A(r) r \frac{\partial n}{\partial r}\right), \tag{14}$$

$$\frac{dS_{k,m,s}}{dt} = \frac{c}{n_G}[\Gamma_{k,m,s} g(\omega_{k,m,s}) - \alpha_{k,m,s}]S_{k,m,s} + \beta_{sp}^{k,m,s} R_{sp}. \tag{15}$$

In the above equations, t stands for time, e is the unit charge, D_A is the ambipolar diffusion coefficient, which generally depend on profiles of both the temperature and carrier concentration [43], $\beta_{sp}^{k,m,s}$ is the spontaneous emission factor for the (k,m,s) mode, $S_{k,m,s}$ is its amplitude, which is directly interrelated with an output laser power P_{out} [with the aid of Eq. (15)], and n_G is the group index of refraction

$$n_G = n_R - \lambda\frac{dn_R}{d\lambda}, \tag{16}$$

where $\lambda = c/\omega$ is the wavelength. G is the carrier generation rate

$$G = \frac{j}{ed_A}, \tag{17}$$

and R is the carrier recombination rate

$$R = R_{nr} + R_{sp} + R_{st}, \tag{18}$$

where R_{nr} is the rate of nonradiative recombination. Both radiative recombination rates for spontaneous (R_{sp}) and stimulated (R_{st}) emission may be expressed as

$$R_{sp} = B(n^{\Gamma} p - n_0^{\Gamma} p_0), \tag{19}$$

$$R_{st} = \frac{c}{\pi n_G r_A^2 d_A} \sum_{k,m,s} S_{k,m,s} \times \int_0^L \int_0^{r_s} \int_0^{2\pi} \left|\psi_{k,m,s}(r,z,\varphi)\right|^2 \times g(\omega_{k,m,s}) r dr dz d\varphi, \tag{20}$$

with B is the radiative recombination coefficient, n^{Γ} is the electron concentration in the Γ conduction band, and the subscript "0" indicating equilibrium values.

A carrier concentration n in the active region plane is reduced in places of the most intense stimulated emission, which immediately decreases a local optical gain g. This phenomenon is called the radial spatial hole burning (SHB) effect. Therefore, for each (k,m,s) mode, effectivity of the radiation amplification in a given VCSEL active region is characterised by the volume confinement factor $\Gamma_{k,m,s}$ describing the correlation between profiles of the mode field intensity and the local gain

$$\Gamma_{k,m,s} g(\omega_{k,m,s}) = \int_0^L \int_0^{r_s} \int_0^{2\pi} g[\omega_{k,m,s}, n(r,z,\varphi), T(r,z,\varphi)] \times \left|\psi_{k,m,s}(r,z,\varphi)\right|^2 r dr dz d\varphi, \tag{21}$$

The optical gain spectrum in the quantum-well (QW) active region may be expressed as [44]

$$g(\omega) = \frac{e^2 M_b^2}{\pi c \varepsilon m_0^2 \omega d_A} \sum_{p,q} \int \left|\langle \psi_{cp} | \psi_{vq} \rangle\right|^2 \times P_{pq}(k) \ell [E_p(k) - E_q(k) - \hbar\omega] \times \{f^c[E_p(k)] - f^v[E_q(k)]\} dk, \tag{22}$$

where k is the wave vector, m_0 is the rest mass of electron, M_b stands for the optical matrix element, Ψ_c and Ψ_v are the envelope wave functions for recombining electrons and holes, respectively, P is the unpolarisation factor, ℓ is the broadening factor (Lorentzian [45] or another [46]), and f^c and f^v are the quasi-Fermi functions for electrons in the conduction band and the valence band, respectively. The summation is carried out over all p conduction bands and q valence bands with E_p and E_q standing for the p^{th}-electron and the q^{th}-hole subband-edge energies, respectively. In multiple-quantum-well (MQW) devices, gain nonuniformity among QWs [47] should be additionally taken into account. Simple relations for the maximal gain directly proportional to the carrier concentration (mostly in broad-area lasers) or to its logarithm (in QW ones) have been often used in diode laser simulations. It may be justified in EELs, where practically always a wavelength of one of longitudinal modes is very close to the maximal-gain position but it may be hardly applied to VCSELs where usually only one longitudinal mode is excited, not necessary close to the gain maximum (c.f. Section 2). Besides, this wavelength position is shifted with temperature and/or operation current.

In the calculations, very important influences of the distributions of both temperature $T(r,z,\varphi)$ and free carrier concentration $n_{fc}(r,z,\varphi)$ on profiles of both real and imaginary parts of the complex index of refraction should be included

$$N_R(r,z,\varphi) = n_R(r,z,\varphi) + \frac{dn_R}{dT}\Big|_{r,z,\varphi}[T(r,z,\varphi) - T_R] + \frac{dn_R}{dn_{fc}}\Big|_{r,z,\varphi} n_{fc}(r,z,\varphi) - i\frac{\alpha(r,z,\varphi) - g(r,z,\varphi)}{2k_0}, \tag{23}$$

where $n_R(r,z,\varphi)$ symbolises a distribution of the real index of refraction at the reference temperature T_R (equal usually to that of the ambient) and without carriers, n_{fc} stands for the free carrier concentration (electrons or holes or both) and $g(r,z,\varphi)$ and $\alpha(r,z,\varphi)$ are temperature dependent distributions of optical gain and optical losses, including free-carrier absorption, intervalence absorption, scattering losses, diffraction losses and so on, but not the band-to-band absorption within the active region which has been already taken into account in the gain calculations. Derivatives dn_R/dT and dn_R/dn_{fc} depend on a local material and temperature. The above simple relation (23) carries information about many interrelations between various physical phenomena including the index guiding (IG) mechanisms with the thermal waveguiding (TW) effect (second term) and the self-focusing (SF) effect (third term) as well as the gain-guiding (GG) mechanism (last term). Additionally, in more advanced VCSEL designs with built-in waveguiding effects, profiles of $n_R(r,z,\varphi)$ and $\alpha(r,z,\varphi)$ may contain designed fixed distributions of an index of refraction and/or absorption, respectively, intentionally introduced in a control way into a resonator volume to stabilise VCSEL waveguiding properties. Then temperature- and carriers-dependent changes of both parts of the complex index of refraction (i.e. the TW, SF, and GG effects) have nearly insignificant influence on a radiation field that is mostly governed by a stable built-in waveguide.

Mutual interactions between physical phenomena may be even more involved. For example, let us consider consequences of a local decrease in a current density. Obviously, it is followed by an analogous decrease in a carrier concen-

tration, which, as an effect of a self-focusing phenomenon, causes an increase in local radiation intensity, additionally decreasing diffraction losses and a lasing threshold. At the same time, a current spreading in this area is modified because of both more intense local stimulated emission and additional diffusion currents. This, in turn, is influencing distributions of local heat sources associated with the Joule heating, nonradiative recombination and absorption of laser radiation, which, because of temperature dependencies of an index of refraction (thermal focusing) and absorption coefficients, is also modifying profiles of radiation intensity again influencing lasing threshold. The above effect is especially important for stimulated radiation, whose standing waves will shift positions of their nodes and anti-nodes, which will affect strongly a distribution of carrier concentrations because of the longitudinal spatial hole burning effect. Modified temperature distributions are additionally affecting current spreading phenomenon because of a temperature dependence of electrical resistivities and additional current components stimulated by temperature gradients etc. etc. Even simingly insignificant change of any profile of a current density, a carrier concentration, temperature and/or radiation intensity is affecting remaining profiles via complex network of mutual nonlinear interactions between them. Hence operation of any VCSEL design and its performance characteristics are very sensitive to details of the device structure. Therefore any advanced simulation of a VCSEL performance should include as many as possible above interactions to be exact, a complex equation system describing individual physical phenomena should include terms or parameters expressing these interrelations.

6. The steady-state solution

For the steady-state condition, Eq. (15) may be easily solved giving the amplitude for the (k,m,s) mode in the following form

$$S_{k,m,s} = \frac{\beta_{sp}^{k,m,s} R_{sp}}{\frac{c}{n_G}[\alpha_{k,m,s} - \Gamma_{k,m,s} g(\omega_{k,m,s})]}, \qquad (24)$$

when the denominator of the above relation is equal to zero, the lasing threshold condition is obtained.

The total laser output power P_{out} emitted by the laser through both its resonator mirrors may be expressed as

$$P_{out} = \frac{c}{n_G} \sum_{k,m,s} (\hbar\omega_{k,m,s}) S_{k,m,s} \times \int_0^{r_z} \int_0^{2\pi} \left|\psi_{k,m,s}(r, z+L, \varphi)\right|^2 \alpha_{k,m,s}^{end}(r)\, r dr d\varphi, \qquad (25)$$

where $\alpha_{k,m,s}^{end}$ stands for the end losses coefficient

$$\alpha_{k,m,s}^{end} = \frac{1}{2L_{k,m,s}} \ln\left(\frac{1}{R_F^{k,m,s} R_R^{k,m,s}}\right), \qquad (26)$$

where L is the resonator length, and R_F and R_R is the power reflectivity coefficients from the front (output) and the rear resonator mirrors, which all generally may be different for different modes and even for different radii r.

7. Conclusions

Fundamental principles of an optical modelling of an operation of VCSELs are given in the present paper. They may be used to formulate optical models of VCSELs or optical parts in more advanced self-consistent models of those devices.

In standard optical simulations developed for typical VCSEL designs operating not very far over their thresholds, simplified scalar approaches are usually used. This possibility is a direct consequence of polarisation properties of VCSEL emitted output beams observed usually just over their lasing thresholds. However, in more advanced VCSEL models, fully vectorial optical approaches are necessary to keep required accuracy. This is especially important in modelling highly-excited VCSELs and/or small-size VCSEL devices (i.e. microresonator lasers), when the assumption of a plane wave propagation inside VCSEL resonators justifying application of scalar approaches is not valid any more.

In the next part [2] of this work, examples of both scalar and vectorial optical models of VCSEL operations will be given. Some approximated and easily used optical VCSEL models will be also presented.

Acknowledgements

This work was supported by the Polish State Committee for Scientific Research (KBN) under the grant # 8-T11B-018-12, by the Marie Curie-Skłodowska Foundation under the grant # MEN/NSF-98-336, and by the CFD Research Corporation, Huntsville, Alabama, USA.

References

1. W. Nakwaski, "Thermal aspects of efficient operation of vertical-cavity surface-emitting lasers", *Opt. Quantum Electron.* **2**, 335–352 (1996).
2. W. Nakwaski, "Simulation of optical phenomena in vertical-cavity surface-emitting lasers. II. Models", *Opto-Electr. Rev.* **8**, this issue.
3. F. Koyama, S. Kinoshita, and K. Iga, "Room-temperature continuous wave lasing characteristics of a GaAs vertical cavtiy surface-emitting laser", *Appl. Phys. Lett.* **55**, 221–222 (1989).
4. W. Nakwaski and M. Osiński, "Thermal properties of vertical-cavity surface-emitting semiconductor lasers", *Progress in Optics* **38**, 165–262 (1998).

5. L. Jewell, S.L. McCall, Y.H. Lee, A. Scherer, A.C. Gossard, and J.H. English, "Lasing characteristics of GaAs microresonators", *Appl. Phys. Lett.* **54**, 1400–1402 (1989).
6. C.J. Chang-Hasnain, J.P. Harbison, L.T. Florez, and N.G. Stoffel, "Polarisation characteristics of quantum well vertical cavity surface emitting lasers", *Electron. Lett.* **27**, 163–165 (1991).
7. Z.G. Pan, S. Jiang, M. Dagenais, R.A. Morgan, K. Hojima, M.T. Asom, and R.E. Leibenguth, "Optical injection induced polarisation bistability in vertical-cavity surface-emitting lasers", *Appl. Phys. Lett.* **63**, 2999–3001 (1993).
8. K.D. Choquette, D.A. Richie, and R.E. Leibenguth, "Temperature dependence of gain-guided vertical-cavity surface emitting laser polarisation", *Appl. Phys. Lett.* **64**, 2062–2064 (1994).
9. K.D. Choquette and R.E. Leibenguth, "Control of vertical-cavity laser polarisation with anisotropic transverse cavity geometries", *IEEE Photon. Technol. Lett.* **6**, 40–42 (1994).
10. T. Mukaihara, N. Hayashi, N. Hatori, F. Koyama, and K. Iga, "Excess intensity noise originated from polarisation fluctuation in vertical-cavity surface-emitting lasers", *IEEE Photon. Technol. Lett.* **7**, 1113–1115 (1995).
11. M. Shimizu, F. Koyama, and K. Iga, "Polarisation characteristics of MOCVD grown GaAs/GaAlAs CBH surface emitting laser", *Jpn. J. Appl. Phys.* **27**, 1774–1775 (1988).
12. S. Jiang, Z. Pan, M. Dagenais, R.A. Morgan, and K. Kojima, "High-frequency polarisation self-modulation in vertical-cavity surface-emitting lasers", *Appl. Phys. Lett.* **63**, 3545–3547 (1993).
13. A.K. Jansen van Doorn, M.P. van Exter, and J.P. Woerdman, "Effects of transverse anisotropy on VCSEL spectra", *Electron. Lett.* **30**, 1941–1943 (1994).
14. C.J. Chang-Hasnain, J.P. Harbison, G. Hasnain, A.C. Von Lehmen, L.T. Florez, and N.G. Stoffel, "Dynamics, polarisation, and transverse mode characteristics of vertical-cavity surface-emitting lasers", *IEEE J. Quantum Electron.* **QE-27**, 1402–1409 (1991).
15. U. Fiedler, G. Reiner, P. Schnitzer, and K.J. Ebeling, "Top surface-emitting vertical-cavity laser diodes for 10–Gb/s data transmission", *IEEE Photon. Technol. Lett.* **8**, 746–748 (1996).
16. T. Ohtoshi, T. Kuroda, A. Niwa, and S. Tsui, "Dependence of optical gain on crystal orientation in surface-emitting lasers with strained quantum wells", *Appl. Phys. Lett.* **65**, 1886–1887 (1994).
17. M. Takahashi, P. Vaccaro, K. Fujita, T. Watanabe, T. Mukaihara, F. Koyama, and K. Iga, "An InGaAs-GaAs vertical-cavity surface-emitting laser grown on GaAs (311)A substrate having low threshold and stable polarisation", *IEEE Photon. Technol. Lett.* **8**, 737–739 (1996).
18. K. Tateno, Y. Ohiso, C. Amano, A. Wakatsuki, and T. Kurokawa, "Growth of vertical-cavity surface-emitting laser structures on GaAs (311)B substrates by metalorganic chemical vapor deposition", *Appl. Phys. Lett.* **70**, 3395–3397 (1997).
19. A. Mizutani, N. Hatori, N. Nishiyama, F. Koyama, and K. Iga, "MOCVD grown InGaAs/GaAs vertical cavity surface emitting laser on GaAs (311)B substrate", *Electron. Lett.* **33**, 1877–1878 (1997).
20. N. Nishiyama, A. Mizutani, N. Hatori, M. Arai, F. Koyama, and K. Iga, "Single-transverse mode and stable-polarisation operation under high-speed modulation of InGaAs-GaAs vertical-cavity surface-emitting laser grown on GaAs (311)B substrate", *IEEE Photon. Technol. Lett.* **10**, 1676–1678 (1998).
21. H. Uenohara, K. Tateno, T. Kagawa, Y. Ohiso, H. Tsuda, T. Kurokawa, and C. Amano, "Investigation of data transmission characteristics of polarisation-controlled 850 nm GaAs-based VCSELs grown on (311)B substrates", *Electron. Lett.* **35**, 45–46 (1999).
22. M. Shimizu, T. Mukaihara, F. Koyama, and K. Iga, "Polarisation control for surface emitting lasers", *Electron. Lett.* **27**, 1067–1069 (1991).
23. K.D. Choquette, R.P. Schneider, Jr., K.L. Lear, and R.E. Leibenguth, "Gain-dependent polarisation properties of vertical-cavity lasers", *IEEE J. Selected Topics Quantum Electron.* **1**, 661–666 (1995).
24. T. Mukaihara, F. Koyama, and K. Iga, "Polarisation control of surface emitting lasers by anisotropic biaxial strain", *Jpn. J. Appl. Phys.* **31**, 1389–1392 (1992).
25. T. Mukaihara, F. Koyama, and K. Iga, "Engineered polarisation control of GaAs/AlGaAs surface emitting lasers by anisotropic stress from elliptical etched substrate hole", *IEEE Photon. Technol. Lett.* **5**, 133–135 (1993).
26. H. Saito, K. Nishi, S. Sugou, and Y. Sugimoto, "Controlling polarisation of quantum-dots surface-emitting lasers by using structurally anisotropic self-assembled quantum dots", *Appl. Phys. Lett.* **71**, 590–592 (1997).
27. T. Yoshikawa, K. Kosaka, K. Kurihara, M. Kajita, Y. Sugimoto, and K. Kasahara, "Complete polarisation control of 8×8 vertical-cavity surface-emitting laser matrix array", *Appl. Phys. Lett.* **66**, 908–910 (1995).
28. T. Yoshikawa, H. Kosaka, M. Kajita, K. Kurihara, Y. Sugimoto, and K. Kasahara, "Alternately perpendicular polarisation in chequer-pattern matrix array of VCSEL's", *Electron. Lett.* **31**, 1573–1574 (1995).
29. T. Yoshikawa, T. Kawakami, H. Saito, H. Kosaka, M. Kajita, K. Kurihara, Y. Sugimoto, and K. Kasahara, "Polarisation-controlled single-mode VCSEL", *IEEE J. Quantum Electron.* **34**, 1009–1015 (1998).
30. D.V. Kuksenkov, H. Temkin, and T. Yoshikawa, "Dynamic properties of vertical-cavity surface-emitting lasers with improved polarisation stability", *IEEE Photon. Technol. Lett.* **8**, 977–979 (1996).
31. K.D. Choquette, K.L. Lear, R.E. Leibenguth, and M.T. Asom, "Polarisation modulation of cruciform vertical-cavity laser diodes", *Appl. Phys. Lett.* **64**, 2767–2769 (1994).
32. M. San Miguel, Q. Feng, and J.V. Moloney. "Light-polarisation dynamics in surface-emitting semiconductor lasers", *Phys. Rev. A* **52**, 1728–1739 (1995).
33. J. Martin-Regalado, M. San Miguel, and N.B. Abraham, "Polarisation switching in quantum-well vertical-cavity surface-emitting lasers", *Opt. Lett.* **21**, 351–353 (1996).
34. J. Martin-Regalado, M. San Miguel, N.B. Abraham, and F. Prati, "Polarisation state selection and switching in VCSEL's", *Proc. SPIE* **2693**, 213–220 (1996).
35. J. Martin-Regalado, S. Balle, and M. San Miguel, "Polarisation and transverse mode dynamics of gain-guided vertical-cavity surface-emitting lasers", *Opt. Lett.* **22**, 460–462 (1997).

36. J. Martin-Regalado, F. Prati, M. San Miguel, and N.B. Abraham, "Polarisation properties of vertical-cavity surface-emitting lasers", *IEEE J. Quantum Electron.* **33**, 765–783 (1997).
37. Y. Yamamoto, S. Machida, and G. Björk, "Microcavity semiconductor laser with enhanced spontaneous emission", *Phys. Rev. A* **44**, 657–667 (1991).
38. T. Baba, T. Hamano, F. Koyama, and K. Iga, "Spontaneous emission factor of a microcavity DBR surface-emitting laser", *IEEE J. Quantum Electron.* **27**, 1347–1358 (1991).
39. I. Vurgaftman and J. Singh, "Steady-state performance of microcavity surface-emitting lasers with quantum confinement of electrons and photons", *Appl. Phys. Lett.* **64**, 1472–1474 (1994).
40. D. Burak and R. Binder, "Electromagnetic characterisation of vertical-cavity surface-emitting lasers based on a vectorial eigenmode calculation", *Appl. Phys. Lett.* **72**, 891–893 (1998).
41. C. Tsao, *Optical Fibre Waveguide Analysis*, Chapter 5.1, Oxford University Press, Oxford, 1992.
42. D. Marcuse, *Light Transmission Optics*, Chapter 1.3, Van Nostrand Reinhold Company, New York, 1982.
43. R.P. Sarzała and W. Nakwaski, "Carrier diffusion inside active regions of gain-guided vertical-cavity surface-emitting lasers", *IEE Proc.-Optoelectron.* **144**, 421–425 (1997).
44. S.F. Yu, "Dynamic behaviour of vertical-cavity surface-emitting lasers", *IEEE J. Quantum Electron.* **32**, 1168–1179 (1996).
45. R.W.H. Engelmann, C.L. Shieh, and C. Shu, "Multiquantum well lasers: Threshold considerations", in *Quantum Well Lasers*, edited by P.S. Zory Jr., Academic Press, Boston, 1993.
46. P.G. Eliseev, "Line shape function for semiconductor laser modelling", *Electron. Lett.* **33**, 2046–2048 (1997).
47. N. Tessler, R. Nagar, G. Eisenstein, S. Chandrasekhar, C.H. Joyner, A.G. Dentai, U. Koren, and G. Reybon, "Nonequilibrium effects in quantum well lasers", *Appl. Phys. Lett.* **61**, 2383–2385 (1992).

